

Total flavone extract from *Ampelopsis megalophylla* induces apoptosis in the MCF-7 cell line

CHUN GUI^{1*}, CHAO ZHANG^{1*}, XIAOMEI XIONG¹, JING HUANG¹, JUAN XI²,
LING GONG³, BISHENG HUANG³ and XIUQIAO ZHANG³

¹The Medicinal Plant Garden; Departments of ²Clinical Biochemistry and ³Pharmacognosy,
School of Laboratory Medicine, Hubei University of Chinese Medicine, Wuhan, Hubei 430065, P.R. China

Received February 19, 2020; Accepted December 9, 2020

DOI: 10.3892/ijo.2021.5172

Abstract. *Ampelopsis megalophylla* has been found to demonstrate anticancer activities in human cancer cells; however, the effect of total flavone extract (TFE), commonly used in Traditional Chinese Medicine, remains unclear. Furthermore, there is limited information on its effects on breast cancer cell lines. The present study aimed to investigate the inhibitory effects of TFE in different human cancer cell lines. In addition, the underlying mechanisms and the signaling pathways involved were also investigated by determining tumor cell morphological changes, and differences in the cell cycle, apoptosis, mitochondrial transmembrane potential, and related protein expression levels in a breast cancer cell line. It was found that TFE inhibited proliferation in seven cancer cell lines (HeLa, A549, MCF-7, HepG2, A2780, SW620 and MDA-MB-231 and demonstrated a strong inhibitory effect on MCF-7 cell proliferation. Cell morphological changes were also observed and arrested at the G₂/M phase following treatment with TFE at different concentrations. In addition, TFE disrupted the mitochondrial membrane potential and upregulated the expression level of apoptotic proteins, including caspase-3, -8 and -9, the Bax/Bcl-2 ratio, and Apaf-1 in time-dependent manner. These results indicated that TFE induced apoptosis of the MCF-7 cells via a mitochondrial-mediated apoptotic pathway. In conclusion, TFE is potentially effective in treating breast cancer.

Introduction

Cancer is one of the most prevalent public health issues and a lethal disease worldwide, posing a serious hazard to the public (1,2). Based on statistics data available from the Global Burden of Diseases, in 2018, ~18,100,000 new cancer cases were diagnosed globally, and nearly a quarter of new cancer cases in women worldwide are breast cancer (3). Furthermore, breast cancer has become the most common malignancy in Chinese women, with an estimated 272,000 women diagnosed and ~70,000 cancer-associated deaths per year (4,5). Alcohol abuse, obesity, a lack of exercise, a later pregnancy or infertility and artificial feeding have been reported to have a marked effect on breast cancer incidence (5).

Currently, the available breast cancer therapeutic strategies include surgery, chemotherapy, radiotherapy, and their combinations (6). However, the therapeutic effects are still limited, particularly with triple-negative and advanced breast cancer. Therefore, novel therapies or new and effective drugs are urgently required for patients with metastatic breast cancer (7). Previous studies have reported that natural medicines could be utilized in breast cancer therapy (8). Compounds, such as cordycepin, quercetin, berberine, polyphenols, and neem seed oil have shown antitumor effects in human breast cancer cells (9-13). Studies have shown that cordycepin could induce cancer cell death by inhibiting RNA synthesis and DNA double-strand breaks (11). Neem seed oil inhibited breast cancer cell growth by inducing apoptosis and cell cycle arrest at G₁ stage (13).

Ampelopsis megalophylla Diels et Gilg (*A. megalophylla*) is a Chinese traditional herb, which is used as a folk medicine. Its tender leaves and stems are commonly used as a herbal tea and to prevent hypertension, particularly in the west of Hubei province (14). Pharmacological research has suggested that *A. megalophylla* has hypertensive, antiinflammatory, antiviral, antitumor, hyperglycemic, antimicrobial, hepatoprotective, neuroprotective, and antioxidant activities (15-17). Notably, its principal effective components are flavonoids and total flavone extract (TFE), which contains compounds, such as ampelopsin, myricetin and myricitrin. TFE was extracted and isolated from *A. megalophylla* using the percolation method (18). Statistically, ampelopsin inhibited cell growth and induced apoptosis in the MCF-7, MDA-MB-231, HepG2, PC-3, EJ, A549, MG-63, HCT-116 and

Correspondence to: Professor Bisheng Huang or Professor Xiuqiao Zhang, Department of Pharmacognosy, School of Laboratory Medicine, Hubei University of Chinese Medicine, Wuhan, 16 Huangjiahu West Road, Hubei 430065, P.R. China
E-mail: hbsh1963@163.com
E-mail: qiaoxzh2000@163.com

*Contributed equally

Key words: TFE, MCF-7 cells, apoptosis, mitochondria pathway

HCT-8 cell lines (19-25). Notably, our previous study found that ampelopsin induced apoptosis in the HeLa cell line by the mitochondrial signaling pathway (15). In addition, myricetin has been widely investigated and demonstrated to have effective anticancer activity (cell proliferation) in several types of cancer, including papillary thyroid, anaplastic thyroid, ovarian, colon, prostate, breast, liver, and lung cancers (26-33). Furthermore, a high number of flavones have been reported to exhibit antitumor effects in different types of cancer cells (33-38). For example, the flavonoid components of *Radix Tetrastigma Hemsleyani* and *Hippophae rhamnoides* have demonstrated anti-proliferative activity in lung cancer cells (34,35). The total flavones of *Choerospondias axillaris* improved ischemia/reperfusion-induced apoptosis via the MAPK signaling pathway (38). Based on these reports, it has been suggested that total flavones are a promising candidate for treating malignancies (39). We hypothesized that TFE may inhibit tumor cell proliferation and in the present study, its antitumor activity and underlying molecular mechanisms in breast cancer cell lines was investigated *in vitro*.

Materials and methods

Chemistry and reagents. DMEM (cat. no. AC10253739), RPMI-1640 (cat. no. AC13431275), 100 IU/ml streptomycin and 100 IU/ml penicillin (cat. no. J180014) and FBS (cat. no. 42G9072K), were purchased from Thermo Fisher Scientific, Inc.. Newborn bovine serum (NBS; cat. no. 11011-7811) was obtained from Hangzhou Sijiqing Biological Engineering Materials Co., Ltd.. The Annexin V-FITC (cat. no. KGA108) apoptosis detection kit was procured from the Nanjing Jiancheng Bioengineering Institute. MTT (cat. no. M-2128), Hoechst 33258, PI (cat. no. P-4170), Rhodamine 123 (Rh 123; cat. no. C2007) were purchased from Sigma-Aldrich (Merck KGaA). Cleaved-caspase-8 (43 kDa; cat. no. ab32351), Bcl-2-associated X protein (Bax; 20 kDa; cat. no. ab25901), B-cell lymphoma-2 (Bcl-2; 26 kDa; cat. no. ab202068), apoptotic protease activating factor-1 (Apaf-1; 135 kDa; cat. no. ab692), caspase-9 (49 kDa; cat. no. ab32539), cleaved-caspase-9 (37 kDa; cat. no. ab133504), and cleaved-caspase-3 (17 kDa; cat. no. ab2000) were all purchased from Abcam. Caspase-3 (30 kDa; cat. no. 14220T) and caspase-8 (43 kDa; cat. no. 4790T) were all purchased from Cell Signaling Technology Inc.. GAPDH (36 kDa; cat. no. 60004-1-Ig) was purchased from ProteinTech Group, Inc.

Cell lines and culture. The HeLa, A549, MCF-7, A2780, SW620 cell lines, and the liver cancer cell line, HepG2 were purchased from the China Center for Typical Culture Collection. The MDA-MB-231 cells were purchased from Procell Life Science and Technology Co., Ltd.. The HeLa cells were cultured in DMEM supplemented with 10% (v/v) NBS, 100 µg/ml streptomycin, and 100 IU/ml penicillin at 37°C in a humidified incubator with 5% CO₂. The A549 cells were maintained in RPMI-1640, supplemented with 10% (v/v) FBS, while the MCF-7, HepG2, A2780, SW620, MDA-MB-231 cells were maintained in DMEM supplemented with 10% (v/v) FBS.

Plant materials. *A. megalophylla* was collected from Laifeng (Hubei, China), which is a county in Hubei province, rich in

natural resources and open for the public, and was identified by Professor Xiuqiao Zhang, Department of Pharmacognosy, School of Pharmaceutical Sciences, Hubei University of Chinese Medicine (Wuhan, China). The plant materials were air-dried and the samples (100 g dry weight) were soaked in 70% ethanol for 24 h at 25°C. The crude extract was prepared using the percolation method and collected at 2 ml/min, and the alcohol was recovered using decompression. The residual water was volatilized, followed by vacuum drying at 60°C. Finally, TFE was obtained (672.38 mg/g in the preliminary study), as previously described (18).

Cell proliferation assay. Cell proliferation was analyzed using the MTT assay. The HeLa, A549, MCF-7, HepG2, A2780 and SW620 cells were seeded in 96-well plates, at a density of 5x10³ cells per well for 24 h. TFE, at final concentrations of 0, 5, 10, 20, 40, 80, and 100 µg/ml was added to the corresponding wells and incubated for 12, 24 and 48 h. Next, 20 µl MTT (5 mg/ml) was added to each well, incubated for 4 h, then the medium was replaced with dimethyl sulfoxide (DMSO; cat. no. RNBF8134; 100 µl/well), to dissolve the formazan crystals. The optical density (OD) was measured at 490 nm using a microplate reader (Bio-Rad Laboratories, Inc.). The experiment was repeated three times. The cell viability was calculated as cell proliferation inhibition ratio (%)=(1-OD_{treated}/OD_{control}) x100%. Cytotoxicity was expressed as the half-maximal inhibitory concentration (IC₅₀), which was calculated using Excel (v2010; Microsoft Corporation), defined as the concentration of TFE inhibiting cell proliferation by 50%.

Cell apoptosis assay. Apoptotic cells were determined using the Annexin V-FITC apoptosis detection kit. Briefly, the MCF-7 cells were treated with TFE (0, 5, 10, 20 and 30 µg/ml) and 5-fluorouracil (5-Fu; cat. no. E1712174) for 10 h. The cells were collected, washed twice with cold PBS (cat. no. 8118334), then resuspended in 500 µl binding buffer. Finally, 5 µl Annexin V-FITC and 5 µl PI was added to the cells, then left in the dark for 10 min at 37°C. The stained cells were analyzed using a flow cytometer (Accuri C6) and the data was analyzed using the FlowJo software (v10) (both from BD Biosciences).

Morphological changes in the apoptotic cells were examined under a microscope after staining the nuclei with Hoechst 33258. After treatment with TFE (0, 5, 10, 20 and 30 µg/ml) and 5-Fu for 10 h, the cells were washed twice with cold PBS and fixed in methanol/acetic acid (3:1 v/v) for 13 min at room temperature. Next, 500 µl Hoechst 33258 (5 µg/ml) solution was added to each well and incubated in the dark for 30 min for staining at room temperature. Finally, changes in the cell nuclei were observed and images were obtained using a charge-coupled device camera (DP70; Olympus Corporation) attached to a fluorescent microscope (IX51; Olympus Corporation).

Detection of the cell cycle. The MCF-7 cells were treated as aforementioned. To analyze the cell cycle, the cells were washed twice with PBS and fixed with cold 75% ethanol overnight at -20°C. The cells were then labeled with PI (50 µg/ml) in the presence of 0.1% RNase A for 30 min at room temperature. The stained cells were detected using a flow cytometer (Accuri C6) and the DNA content was analyzed using FlowJo software (v10) (both from BD Biosciences).

Table I. The IC₅₀ values in six cell lines following TFE treatment for 12, 24 and 48 h.

Cell lines	IC ₅₀ values, $\mu\text{g/ml}$		
	12 h	24 h	48 h
HeLa	70.27 \pm 2.85	49.11 \pm 1.4 ^a	31.01 \pm 1.93 ^a
A549	59.68 \pm 3.04	43.66 \pm 2.24 ^a	31.77 \pm 3.06 ^a
MCF-7	70.98 \pm 7.04	33.45 \pm 1.09 ^a	27.32 \pm 0.24 ^a
HepG2	80.5 \pm 10.38	79.14 \pm 3.98 ^a	53.05 \pm 3.15 ^a
A2780	43.41 \pm 3.29	22.74 \pm 2.3 ^a	16.98 \pm 1.56 ^a
SW620	55.14 \pm 2.48	42.73 \pm 2.05 ^a	21.39 \pm 1.47 ^a

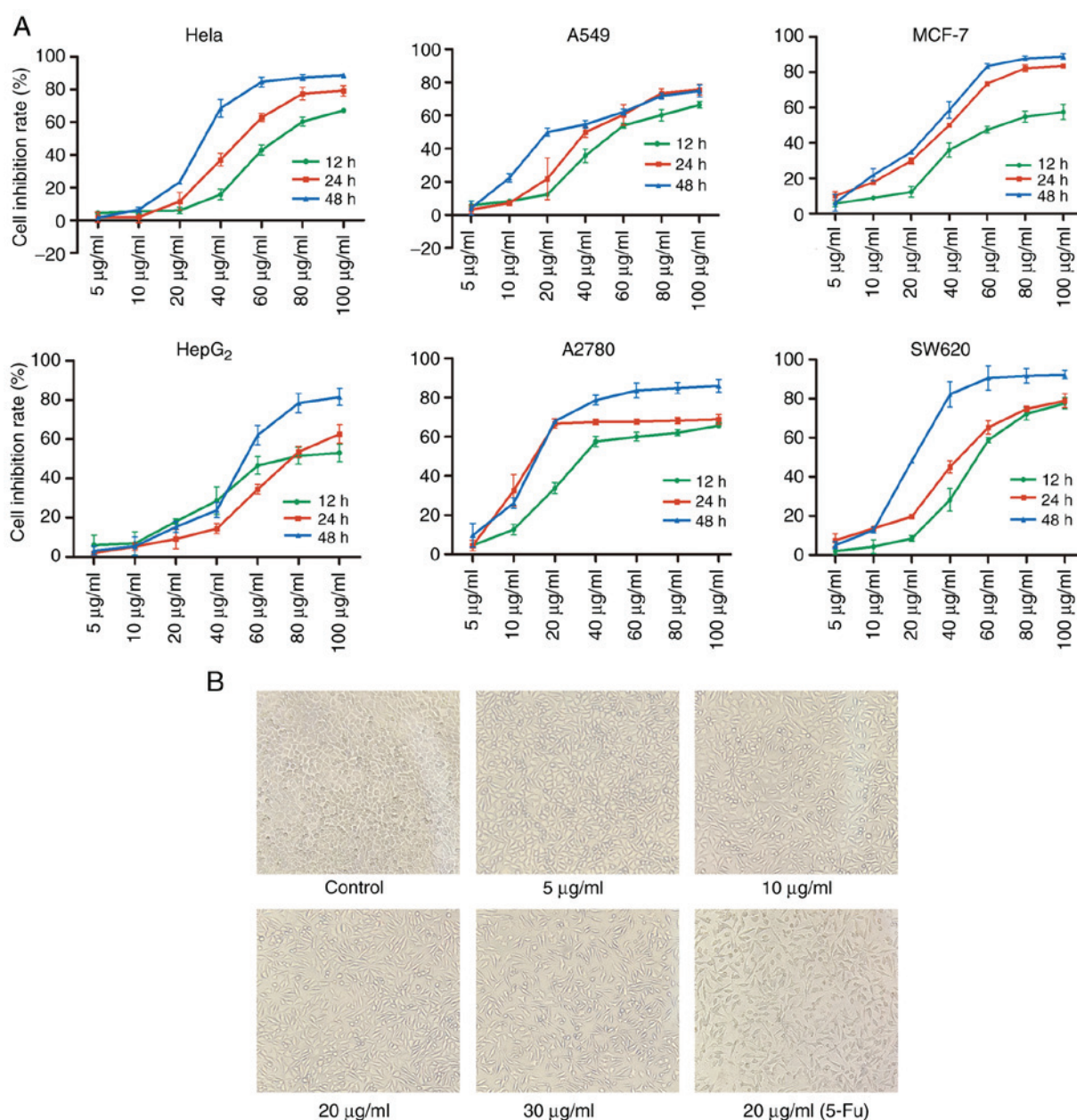
^aP<0.01 vs. 12 h.

Figure 1. Inhibition of cell growth by TFE in six cell lines and morphological changes in the MCF-7 cell line treated with TFE. (A) MTT assay analysis of the inhibition ratio in six cell lines following 12, 24, 48 h treatment with TFE at different concentrations (0, 5, 10, 20, 40, 60, 80 and 100 $\mu\text{g/ml}$). (B) The MCF-7 cells were treated with different concentrations of TFE (0, 5, 10, 20 and 30 $\mu\text{g/ml}$) and 20 $\mu\text{g/ml}$ 5-Fu for 10 h, then observed using a light microscope (magnification, $\times 100$). TFE, total flavone extract; 5-Fu, 5-fluorouracil.

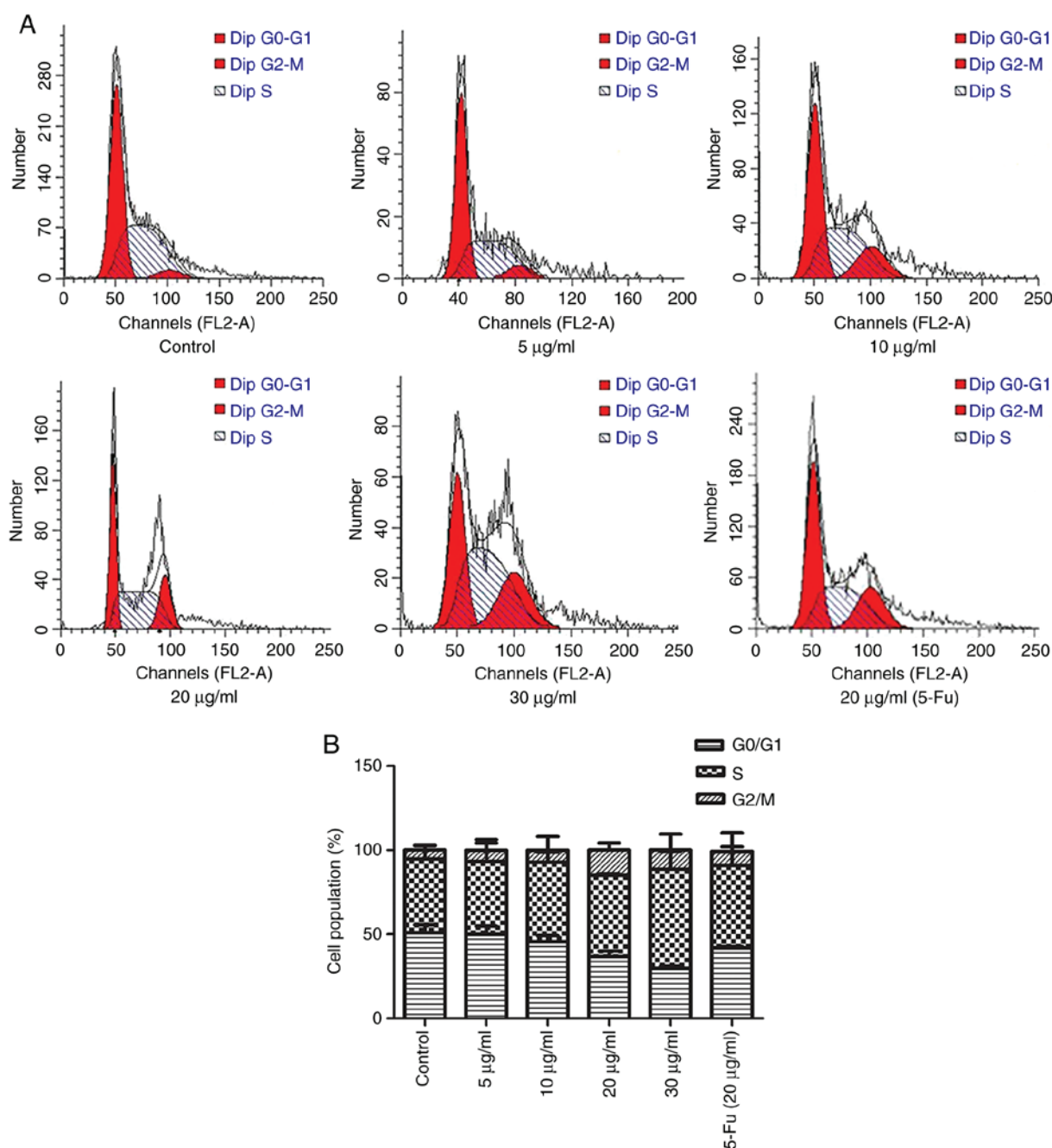


Figure 2. Cell cycle analysis of TFE-treated MCF-7 cells. (A) Cell cycle measurement of the MCF-7 cells following treatment with TFE for 10 h at different concentrations (5, 10, 20 and 30 µg/ml) and 20 µg/ml 5-Fu. (B) Quantification of G₀/G₁, S and G₂/M phases in the TFE-treated MCF-7 cells. The data are presented as the mean ± SD. TFE, total flavone extract; 5-Fu, 5-fluorouracil.

Detection of mitochondrial transmembrane potential ($\Delta\Psi_m$) variation using flow cytometry. The $\Delta\Psi_m$ was determined using Rh-123. The MCF-7 cells were treated with TFE (0, 5, 10, 20 and 30 µg/ml) and 5-Fu for 10 h, harvested, then Rh-123 solution (1.0 µg/ml) was subsequently added to the cells and were incubated at 37°C for 30 min. The results were detected using a flow cytometer (Accuri C6) and analyzed using the FlowJo software (v10) (both from BD Biosciences).

Western blot analysis. For western blot analysis, the TFE-treated MCF-7 cells (0, 5, 10, 20 and 30 µg/ml for 12 h, or with 20 µg/ml for 6, 12, 24 h) were washed twice with PBS and lysed in RIPA lysis buffer (PAB180006; Bioswamp

Wuhan Beinle Biotechnology Co., Ltd.). The cell debris was removed using centrifugation at 13,523 × g for 10 min at 4°C. The supernatant was harvested and the concentration was measured using a BCA protein assay kit (PAB180007; Shanghai, China). Protein samples (10 µg) were separated using 15% SDS-PAGE, performed at 80 V for 40 min, followed by 120 V for 50 min. After separation, the proteins were transferred onto PVDF membranes (IPVH00010; EMD Millipore). The membranes were blocked in TBS-Tween-20 (TBST) buffer containing 5% (w/v) skimmed milk for 1.5 h at room temperature and incubated overnight at 4°C with the primary antibodies (caspase-8, 1:1,000; cleaved-caspase-8, 1:1,000; caspase-9, 1:2,000; cleaved-caspase-9, 1:1,000; caspase-3,

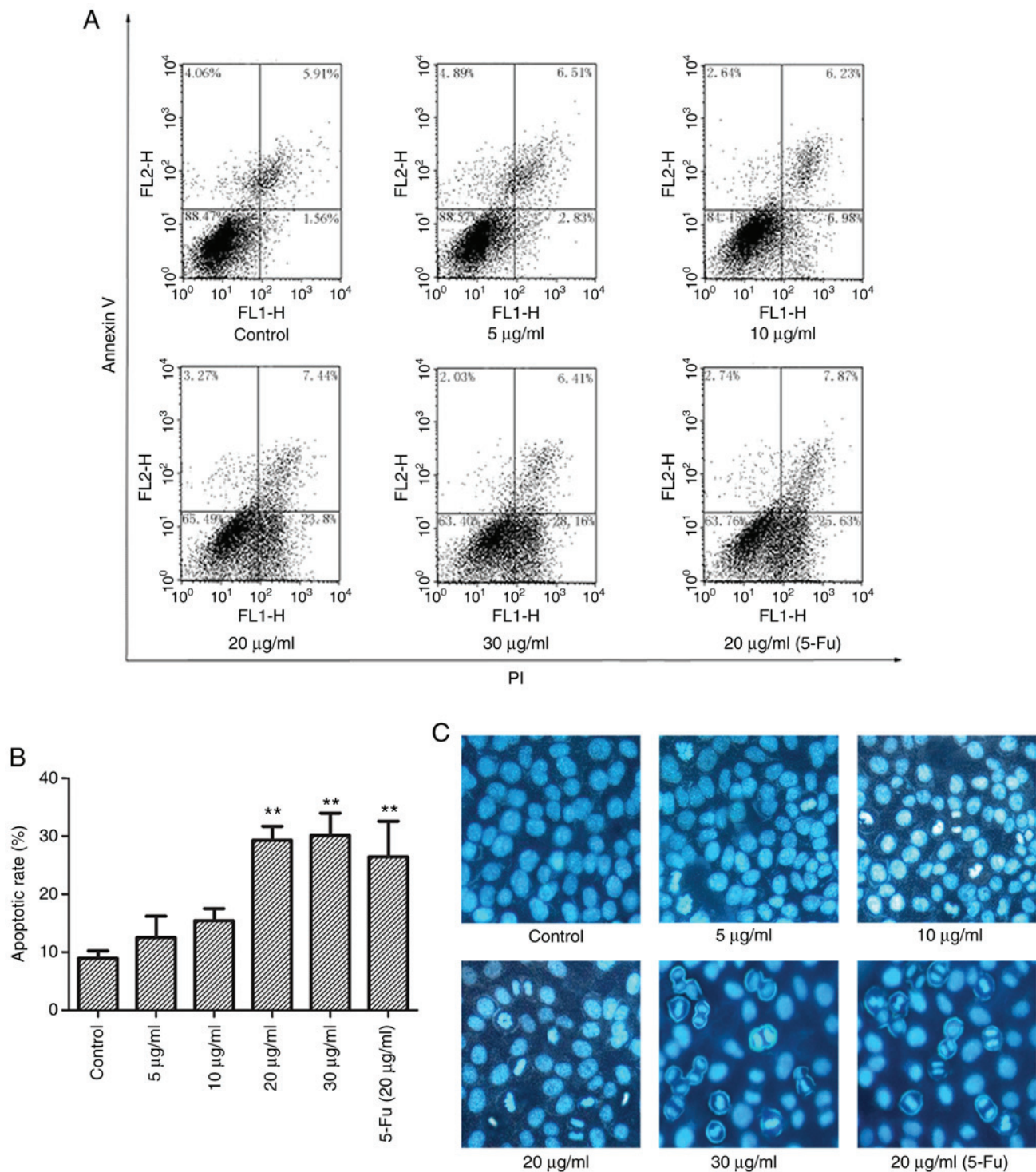


Figure 3. TFE induces MCF-7 cell apoptosis. (A) Representative flow cytometry plots of apoptosis in the TFE-treated (0, 5, 10, 20 and 30 µg/ml) MCF-7 cells and with 20 µg/ml 5-Fu. (B) The apoptotic rate in TFE-treated MCF-7 cells was statistically analyzed. (C) Nuclei staining with Hoechst 33258 in TFE-treated (0, 5, 10, 20 and 30 µg/ml) MCF-7 cells, and with 20 µg/ml 5-Fu. The data are presented as the mean ± SD. **P<0.01. vs. Con. TFE, total flavone extract; 5-Fu, 5-fluorouracil; Con, control.

1:5,000; cleaved-caspase-3, 1:1,000; Bax, 1:1,000; Bcl-2, 1:500; Apaf-1, 1:1,000; GAPDH, 1:5,000) diluted in TBST, followed by incubation with HRP-conjugated secondary antibodies (goat anti-rabbit IgG, PAB160011; 1:10,000; goat anti-mouse IgG, PAB160009; 1:10,000) (both from Bioswamp Wuhan Beinle Biotechnology Co., Ltd.) for 1 h at room temperature. Finally, the signal was developed using an enhanced chemiluminescence plus kit (EMD Millipore) and detected using

the ChemiDoc Touch imaging system (Tanon-5200; Tanon Science and Technology Co., Ltd.). The ImageJ software 1.48v (National Institutes of Health) was used to calculate the relative density of the proteins.

Statistical analysis. All the data are presented as the mean ± SD and analyzed using the SPSS v17.0 (SPSS Inc.). The experiments were performed in triplicate. One-way ANOVA followed

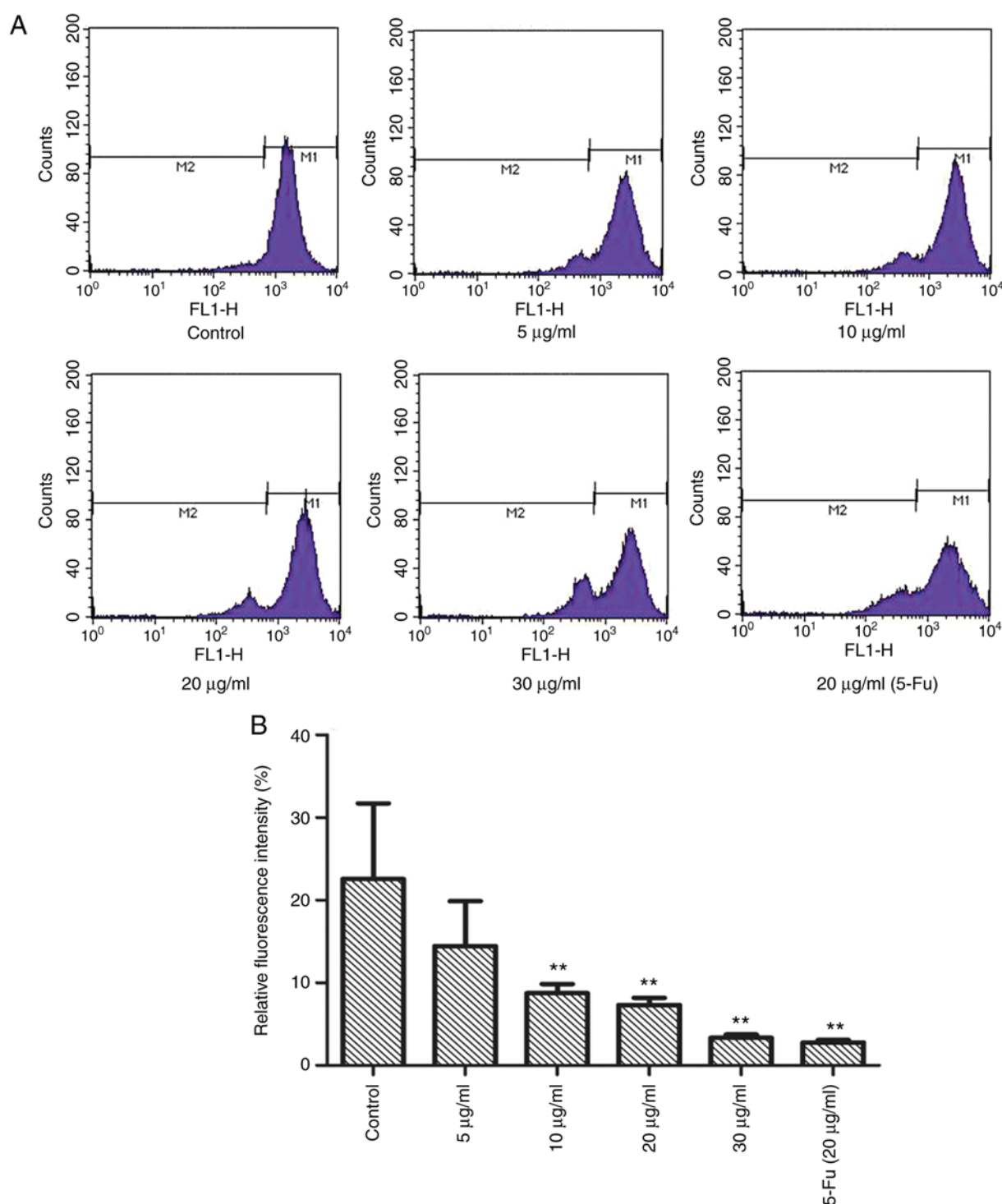


Figure 4. Changes in the mitochondrial transmembrane potential ($\Delta\Psi_m$) in the MCF-7 cells. (A) TFE decreases the relative fluorescence intensity in MCF-7 cells. (B) Quantification of the relative fluorescence intensity in TFE-treated (0, 5, 10, 20 and 30 $\mu\text{g/ml}$) MCF-7 cells, and with 20 $\mu\text{g/ml}$ 5-Fu. The data are presented as the mean \pm SD. ** $P < 0.01$. vs. Con. TFE, total flavone extract; 5-Fu, 5-fluorouracil; Con, control.

by Tukey's post hoc test was used to compare the differences between continuous data (>3 groups), while differences between 2 groups were compared using a Student's t-test. $P < 0.05$ was considered to indicate a statistically significant difference.

Results

TFE inhibits the proliferation of the MCF-7 cells. First, the effect of TFE on the proliferation of the HeLa, A549, MCF-7,

HepG₂, A2780, and SW620 cells was investigated using a MTT assay. It was found that the six types of cell lines treated with TFE (0, 5, 10, 20, 40, 60, 80, and 100 $\mu\text{g/ml}$) at 3 time intervals (12, 24 and 48 h) demonstrated a notable decrease in cell proliferation (Fig. 1A). In particular, the IC₅₀ values were 31.01 ± 1.93 , 31.77 ± 3.06 , 27.32 ± 0.24 , 53.05 ± 3.15 , 16.98 ± 1.56 and 21.39 ± 1.47 $\mu\text{g/ml}$ for HeLa, A549, MCF-7, HepG₂, A2780 and SW620 cells, respectively at 48 h (Table I).

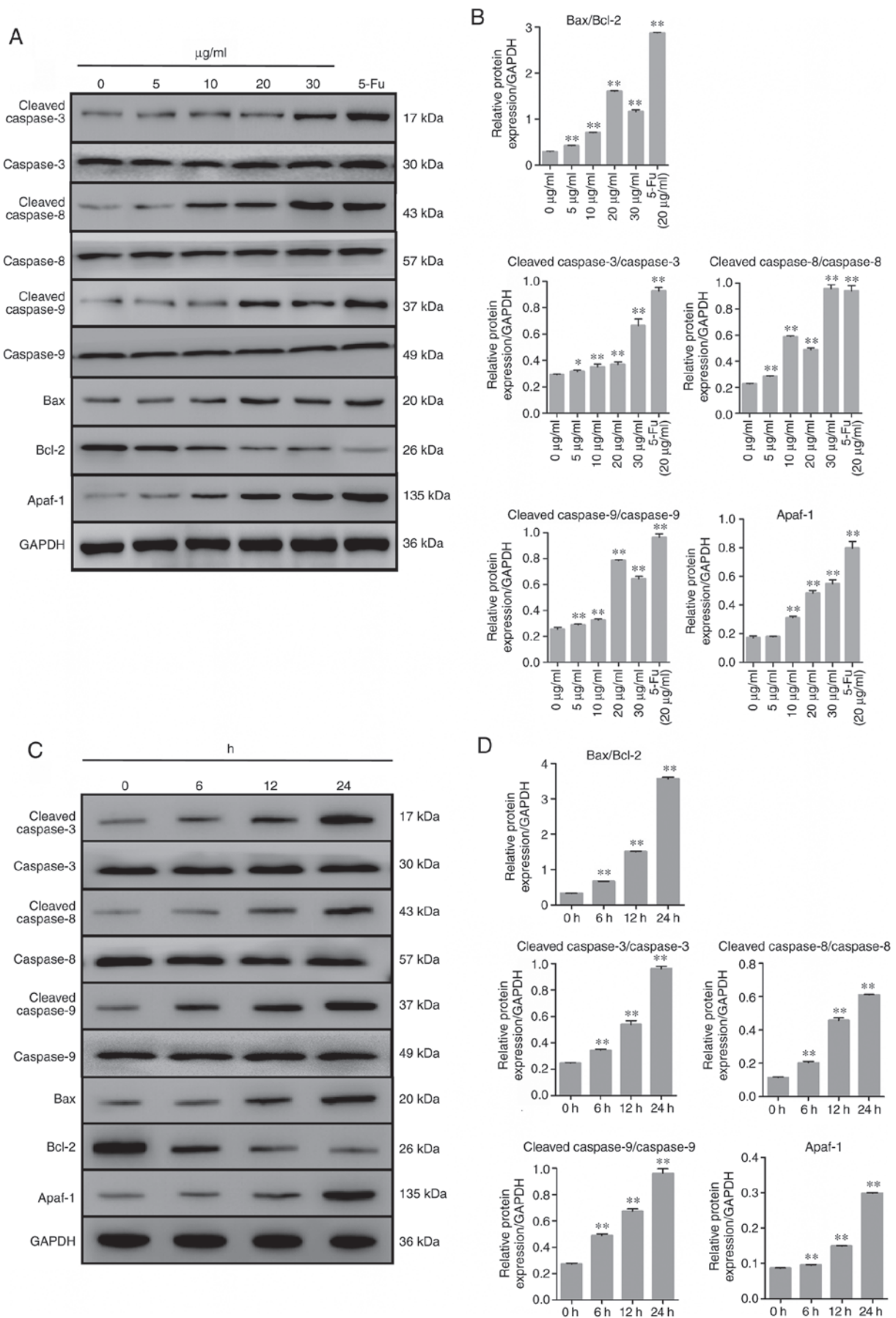


Figure 5. Expression level of the apoptosis-related proteins in TFE-treated MCF-7 cells. (A and C) The relative expression levels of the apoptotic proteins in TFE-treated (0, 5, 10, 20 and 30 µg/ml for 12 h, or with 20 µg/ml for 6, 12, 24 h) MCF-7 cells. (B and D) Quantification of the relative protein expression level in the TFE-treated MCF-7 cells. The data are presented as the mean ± SD. *P<0.05, **P<0.01. vs. Con. TFE, total flavone extract; 5-Fu, 5-fluorouracil; Con, control.

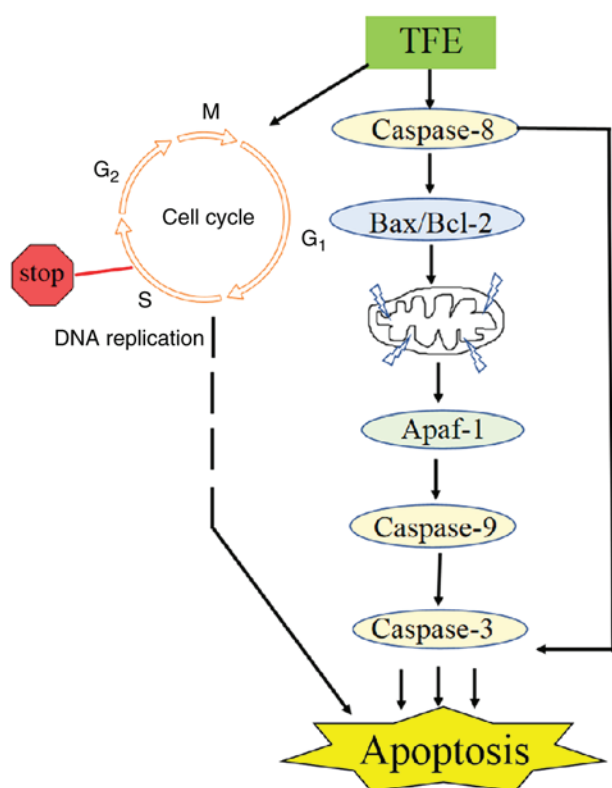


Figure 6. Schematic diagram of the intracellular signaling mechanism during TFE-induced apoptosis in MCF-7 cells. TFE, total flavone extract.

The A2780 and SW620 cells showed sensitivity to TFE treatment compared with that in the MCF-7 cell line. Notably, the mechanism of apoptosis for ampelopsin/myricetin (principal effective components of TFE) have been reported in ovarian and colon cancer (22,32). Therefore, the breast cancer cell line was selected as a priority, as it had not been investigated in this cell line before. To investigate the efficacy of TFE in breast cancer, the MDA-MB-231 cell line was assessed using the MTT assay. The IC_{50} values were $84.74 \pm 0.747\%$ at 48 h.

Furthermore, separately and simultaneously, the cellular morphological changes were observed using light microscopy. Increasing concentrations of TFE, caused cell shrinkage, cell size reduction, sloughing and increased cell death; however, the control cells were normal. Morphological changes (cell shrinkage) were also observed in the positive control (Fu-5-treated) cells (Fig. 1B). Therefore, further experiments were performed using the MCF-7 cell line and TFE concentration between 5 and 30 $\mu\text{g/ml}$.

TFE induces apoptosis of MCF-7 cells. The cell cycle plays a significant role in apoptosis, particularly in the intrinsic mitochondrial-related pathway. Therefore, the effect of TFE treatment on cell cycle arrest in the MCF-7 cell line was investigated using PI staining. The results indicated that the cells were arrested at the G_2/M phase (Fig. 2A). There was a notable increase in the proportion of cells in the G_2/M phase (from 7.64 ± 0.98 to $22.24 \pm 1.43\%$) and a decrease in the number of cells in the G_0/G_1 phase (from 51.79 ± 2.03 to $31.13 \pm 1.03\%$; Fig. 2B) compared with that in the control group. These results

indicated that TFE induced cell cycle arrest in the MCF-7 cells.

Next, it was investigated whether TFE induced apoptosis in the MCF-7 cells. Annexin V-FITC/PI staining was used to evaluate the apoptotic rate of MCF-7 cells following TFE treatment for 10 h. The results showed an increased in the apoptotic rate, and the percentage of apoptotic cells significantly increased from 12.49 ± 3.72 (5 $\mu\text{g/ml}$) to 15.45 ± 2.07 , 29.28 ± 2.45 , and $30.11 \pm 3.87\%$ after treatment with 10, 20 and 30 $\mu\text{g/ml}$ TFE, respectively. The apoptotic rate of the positive control was $26.40 \pm 6.17\%$, whereas in the control cells it was $7.47 \pm 1.24\%$ ($P < 0.05$) (Fig. 3A and B).

To visually observe apoptosis, the MCF-7 cells were treated with TFE and Fu-5 (20 $\mu\text{g/ml}$), then stained with Hoechst 33258. As shown in Fig. 3C, apoptotic morphological changes were observed, including nuclear chromatin condensation and fragmentation, with increase in the light blue fluorescence observed compared with that in the control, and decrease in normal cell number.

TFE $\Delta\Psi_m$ of the MCF-7 cells. Subsequently, it was investigated whether TFE altered the $\Delta\Psi_m$ using Rh-123 staining. As shown in Fig. 4A and B, compared with that in the control cells, with a relative fluorescence intensity of $22.54 \pm 2.16\%$, the MCF-7 cells, treated with different TFE concentrations (5, 10, 20, 30 $\mu\text{g/ml}$), demonstrated decreased relative fluorescence intensity, from 14.44 ± 5.45 to $3.34 \pm 0.41\%$, indicating a notable decrease in $\Delta\Psi_m$.

TFE regulates relative protein expression level in apoptosis. To investigate the possible mechanism of TFE-induced apoptosis in the MCF-7 cells, the expression level of related proteins, including anti-apoptotic Bcl-2, pro-apoptotic Bax and caspase-3. In addition, several other proteins involved in the related pathways were also investigated, such as caspase-8, Apaf-1 and caspase-9. The results, shown in Fig. 5A and C, demonstrated that treatment with TFE decreased the protein expression level of Bcl-2 and increased the expression level of Bax, caspase-3, -8 and -9 and Apaf-1. TFE demonstrated regulatory effects on these apoptosis-related proteins in a time-dependent manner (Fig. 5B and D).

Discussion

Breast cancer, which has been reported to be the most malignant tumor in women, has no specific drug treatment. Furthermore, triple-negative breast cancer is the worst type and has poor therapeutic response due to the lack of specific receptors (25,30). Presently, targeted drugs, such as inhibitors and antagonists are used in clinical practice. However, these types of drugs are susceptible to resistance (7). Currently, an increasing number of natural products are under investigation in cancer research. *A. megalophylla*, is a Chinese traditional herb used as a folk medicine and it has a long history of use in Hubei province. Total flavonoids are the major components extracted from *A. megalophylla* (18).

In the present study, the antitumor activity of TFE in six cancer cell lines (HeLa, A549, MCF-7, HepG2, A2780 and SW620) was investigated using the MTT assay and followed by microscopic observations. Furthermore, the flow

cytometric analysis suggested that TFE notably inhibited tumor cell proliferation and induced apoptosis in the MCF-7 cells.

In addition, these findings were supported by western blot analysis and Rh-123 staining, which revealed the expression of key apoptotic proteins and the change in $\Delta\Psi_m$ induced by TFE. The Bcl-2 family members are critical regulators of apoptosis, including the anti-apoptotic proteins Bcl-2 and pro-apoptotic Bax proteins (33). The increased of Bcl-2 has been associated with the induction of apoptosis by the alteration in $\Delta\Psi_m$ (36). As shown in Fig. 5 there was an upregulation in the Bax/Bcl-2 ratio in TFE-treated MCF-7 cells, indicating apoptosis. Notably, the relative fluorescence intensity was decreased following TFE treatment (Fig. 4). These results indicated that TFE treatment of the MCF-7 cells induced apoptosis, possibly through the mitochondrial pathway.

Apoptosis is a complex process, that involves several signaling pathways (10). Based on the results from the present study, the mitochondrial pathway was the main target of TFE; however, further research is important to elucidate the pathway mediating the effects of TFE in the MCF-7 cells. Subsequently, the caspase family members and mitochondria-related proteins were also investigated to verify that apoptosis occurred and to determine the possible role of this pathway. Caspase-3 activates apoptosis by cleaving a number of cellular proteins and is characteristically proteolyzed during the apoptotic process (37). TFE induced a dose-dependent decrease of $\Delta\Psi_m$ and the expression level of Bcl-2 (Fig. 5). Bcl-2 is expressed in the membranes of the nucleus and endoplasmic reticulum (5). It has been reported that cytochrome *c* sequentially binds to Apaf-1 to stimulate the apoptotic protease cascade, forming an activation complex with caspase-9 and activating caspase-3 (30,33). The activation of pro-caspase-8 cleaves the pro-apoptotic Bcl-2 family member (40). In the current study, TFE treatment significantly upregulated cleaved caspase-8 and Bax, and downregulated Bcl-2 expression level, and promoted Apaf-1 expression level (Fig. 5). Collectively, the results from the present study indicated that treatment with TFE induced caspase-8, which may have directly activated Bax/Bcl-2, caused $\Delta\Psi_m$ loss, and the binding of Apaf-1, to then activate the caspase-9/3 cascade. These effects ultimately induced apoptosis of the MCF-7 cells (Fig. 6).

In the present study, on the one hand the effect of cell cycle stage was only examined; therefore, further investigation is required into the mechanism involved. For example, the expression levels of cell cycle and apoptosis-associated proteins could be detected with immunohistochemistry. On the other hand, to further elucidate the signal pathway in-depth, detailed studies into the mitochondrial apoptosis pathway, the expression level of the cytochrome *c* protein in mitochondria/cytoplasm fractions, and into the activity and mechanism of TFE *in vivo* are also required in the future.

In summary, it was found that TFE inhibited seven cancer cell lines (HeLa, A549, MCF-7, HepG2, A2780, SW620 and MDA-MB-231). These findings indicated that the mitochondria-mediated apoptotic pathway was involved in TFE-induced apoptosis of the MCF-7 cells. Furthermore, the results provided an experimental basis for the use of TFE, as an agent for the treatment of breast cancer. To further elucidate

this signal pathway in-depth, *in vivo* studies are in progress to investigate the activity of TFE.

Acknowledgements

Not applicable.

Funding

This research was supported by the National Natural Science Foundation of China (grant no. 31170335), the Foundation of the Scientific and Technological Bureau of Wuhan (grant no. 2018060401011308) and the Foundation of 'Beanstalk Program' of Hubei University of Chinese Medicine.

Availability of data and materials

The datasets generated and/or analyzed during the present study are available from the corresponding author upon reasonable request.

Authors' contributions

XZ and BH conceived and designed the study. CG, CZ, JH and LG performed all of the experiments. CG and CZ analyzed the data. CZ, XX and JX performed the statistical analysis. CG wrote the manuscript. CG, BH and XZ confirm the authenticity of all the raw data. All authors have reviewed the manuscript and read and approved the final manuscript.

Ethics approval and consent to participate

Not applicable.

Patient consent for publication

Not applicable.

Competing interests

The authors declare that they have no competing interests.

References

1. Siegel RL, Miller KD and Jemal A: Cancer statistics, 2018. *CA Cancer J Clin* 68: 7-30, 2018.
2. Czarnomysy R, Surazyński A, Muszynska A, Gornowicz A, Bielawska A and Bielawski K: A novel series of pyrazole-platinum(II) complexes as potential anti-cancer agents that induce cell cycle arrest and apoptosis in breast cancer cells. *J Enzyme Inhib Med Chem* 33: 1006-1023, 2018.
3. Global Burden of Disease Cancer Collaboration, Fitzmaurice C, Allen C, Barber RM, Barregard L, Bhutta ZA, Brenner H, Dicker DJ, Chimed-Orchir O, Dandona R, *et al*: Global, regional, and national cancer incidence, mortality, years of life lost, years lived with disability, and disability-adjusted life-years for 32 cancer groups, 1990 to 2015: A systematic analysis for the Global Burden of Disease Study. *JAMA Oncol* 3: 524-548, 2017.
4. Fan L, Strasser-Weippl K, Li JJ, St Louis J, Finkelstein DM, Yu KD, Chen WQ, Shao ZM and Goss PE: Breast cancer in China. *Lancet Oncol* 15: e279-e289, 2014.
5. Shi T, Min M, Sun C, Zhang Y, Liang M and Sun Y: Periodontal disease and susceptibility to breast cancer: A meta-analysis of observational studies. *J Clin Periodontol* 45: 1025-1033, 2018.

6. Cao W, Li JQ, Hao QY, Jaydutt VV and Wu Y: AMP-activated protein kinase: A potential therapeutic target for triple-negative breast cancer. *Breast Cancer Res* 21: 29, 2019.
7. Tejashree M and Manu L: From natural products to designer drugs: Development and molecular mechanisms action of novel anti-microtubule breast cancer therapeutics. *Curr Top Med Chem* 17: 2559-2568, 2017.
8. Tsao AS, Kim ES and Hong WK: Chemoprevention of cancer. *CA Cancer J Clin* 54: 150-180, 2004.
9. Alimohammadi M, Lahiani MH, McGehee D and Khodakovskaya M: Polyphenolic extract of InsP 5-ptase expressing tomato plants reduce the proliferation of MCF-7 breast cancer cells. *PLoS One* 12: e175778, 2017.
10. Khorsandi L, Orazizadeh M, Niazvand F, Abbaspour MR, Mansouri E and Khodadadi A: Quercetin induces apoptosis and necroptosis in MCF-7 breast cancer cells. *Bratisl Lek Listy* 118: 123-128, 2017.
11. Lee HJ, Burger P, Vogel M, Friese K and Bruning A: The nucleoside antagonist cordycepin causes DNA double strand breaks in breast cancer cells. *Invest New Drugs* 30: 1917-1925, 2012.
12. Pan Y, Zhang F, Zhao Y, Shao D, Zheng X, Chen Y, He K, Li J and Chen L: Berberine enhances chemosensitivity and induces apoptosis through dose-orchestrated AMPK signaling in breast cancer. *J Cancer* 8: 1679-1689, 2017.
13. Sharma R, Kaushik S, Shyam H, Agarwal S and Balapure AK: Neem seed oil induces apoptosis in MCF-7 and MDA MB-231 human breast cancer cells. *Asian Pac J Cancer Prev* 18: 2135-2140, 2017.
14. Xie X, Wang J and Zhang H: Characterization and antitumor activities of a water-soluble polysaccharide from *Ampelopsis megalophylla*. *Carbohydr Polym* 129: 55-61, 2015.
15. Cheng P, Gui C and Huang J, Xia Y, Fang Y, Da GZ and Zhang XQ: Molecular mechanisms of ampelopsin from *Ampelopsis megalophylla* induces apoptosis in HeLa cells. *Oncol Lett* 14: 2691-2698, 2017.
16. Kou X, Shen K, An Y, Qi S, Dai WX and Yin Z: Ampelopsin inhibits H₂O₂-induced apoptosis by ERK and Akt signaling pathways and up-regulation of heme oxygenase-1. *Phytother Res* 26: 988-994, 2012.
17. Xie XF, Wang JW, Zhang HP, Li QX and Chen BY: Chemical composition, antimicrobial and antioxidant activities of essential oil from *Ampelopsis megalophylla*. *Nat Prod Res* 28: 853-860, 2014.
18. He XY, Yang RJ, Zhu ZK, Jiang C, Zhang XQ and Liu YW: Determination of total flavonoids in different extracts of *Ampelopsis megalophylla*. *Herald Med* 31: 211-212, 2012.
19. Chen XM, Xie XB, Zhao Q, Wang F, Bai Y, Yin JQ, Jiang H, Xie XL, Jia Q and Huang G: Ampelopsin induces apoptosis by regulating multiple c-Myc/S-phase kinase-associated protein 2/F-box and WD repeat-containing protein 7/histone deacetylase 2 pathways in human lung adenocarcinoma cells. *Mol Med Rep* 11: 105-112, 2015.
20. Liu B, Tan X and Liang J, Wu S, Liu J, Zhang Q and Zhu R: ERRATUM: A reduction in reactive oxygen species contributes to dihydromyricetin-induced apoptosis in human hepatocellular carcinoma cells. *Sci Rep* 5: 7940, 2015.
21. Lu M, Huang W, Bao N, Zhou G and Zhao J: The flavonoid ampelopsin inhibited cell growth and induced apoptosis and G0/G1 arrest in human osteosarcoma MG-63 cells in vitro. *Pharmazie* 70: 388-393, 2015.
22. Ni F, Gong Y, Li L, Abdolmaleky HM and Zhou JR: Flavonoid ampelopsin inhibits the growth and metastasis of prostate cancer in vitro and in mice. *PLoS One* 7: e38802, 2012.
23. Park GB, Jeong JY and Kim D: Ampelopsin-induced reactive oxygen species enhance the apoptosis of colon cancer cells by activating endoplasmic reticulum stress-mediated AMPK/MAPK/XAF1 signaling. *Oncol Lett* 14: 7947-7956, 2017.
24. Zhang B, Dong S, Cen X, Wang X, Liu X, Zhang H, Zhao X and Wu Y: Ampelopsin sodium exhibits antitumor effects against bladder carcinoma in orthotopic xenograft models. *Anticancer Drugs* 23: 590-596, 2012.
25. Zhou Y, Liang X, Chang H, Shu F, Wu Y, Zhang T, Fu Y, Zhang Q, Zhu JD and Mi M: Ampelopsin-induced autophagy protects breast cancer cells from apoptosis through Akt-mTOR pathway via endoplasmic reticulum stress. *Cancer Sci* 105: 1279-1287, 2014.
26. Cao J, Chen H, Lu W, Wu Y, Wu X, Xia D and Zhu J: Myricetin induces protective autophagy by inhibiting the phosphorylation of mTOR in HepG2 cells. *Anat Rec (Hoboken)* 301: 786-795, 2018.
27. Ha TK, Jung I, Kim ME, Bae SK and Lee JS: Anti-cancer activity of myricetin against human papillary thyroid cancer cells involves mitochondrial dysfunction-mediated apoptosis. *Biomed Pharmacother* 91: 378-384, 2017.
28. Jo S, Ha TK, Han SH, Kim ME, Jung I, Lee HW, Bae SK and Lee JS: Myricetin induces apoptosis of human anaplastic thyroid cancer cells via mitochondria dysfunction. *Anticancer Res* 37: 1705-1710, 2017.
29. Jose J, Dhanya AT, Haridas KR, Sumesh Kumar TM, Jayaraman S, Variyar EJ and Sudhakaran S: Structural characterization of a novel derivative of myricetin from *Mimosa pudica* as an anti-proliferative agent for the treatment of cancer. *Biomed Pharmacother* 84: 1067-1077, 2016.
30. Knickle A, Fernando W, Greenshields AL, Rupasinghe H and Hoskin DW: Myricetin-induced apoptosis of triple-negative breast cancer cells is mediated by the iron-dependent generation of reactive oxygen species from hydrogen peroxide. *Food Chem Toxicol* 118: 154-167, 2018.
31. Ma L, Cao X, Wang H, Lu K, Wang Y, Tu C, Dai Y, Meng Y, Li Y, Yu P, *et al*: Discovery of myricetin as a potent inhibitor of human flap endonuclease 1, which potentially can be used as sensitizing agent against HT-29 human colon cancer cells. *J Agric Food Chem* 67: 1656-1665, 2019.
32. Ye C, Zhang C, Huang H, Yang B, Xiao G, Kong D, Tian Q, Song Q, Song Y, Tan H, *et al*: The natural compound myricetin effectively represses the malignant progression of prostate cancer by inhibiting PIM1 and disrupting the PIM1/CXCR4 Interaction. *Cell Physiol Biochem* 48: 1230-1244, 2018.
33. Zheng AW, Chen YQ, Zhao LQ and Feng JG: Myricetin induces apoptosis and enhances chemosensitivity in ovarian cancer cells. *Oncol Lett* 13: 4974-4978, 2017.
34. Wang ZR, Wang L, Yin HH, Yang FJ, Gao YQ and Zhang ZJ: Effect of total flavonoids of *Hippophae rhamnoides* on contractile mechanics and calcium transfer in stretched myocyte. *Space Med Eng (Beijing)* 13: 6-9, 2000.
35. Zhong LR, Chen X and Wei KM: *Radix tetragynis* hemsleyana flavone induces apoptosis in human lung carcinoma A549 cells by modulating the MAPK pathway. *Asian Pac J Cancer Prev* 14: 5983-5987, 2013.
36. Gong WY, Wu JF, Liu BJ, Zhang HY, Cao YX, Sun J, Lv YB, Wu X and Dong JC: Flavonoid components in *Scutellaria baicalensis* inhibit nicotine-induced proliferation metastasis and lung cancer-associated inflammation in vitro. *Int J Oncol* 44: 1561-1570, 2014.
37. Li-Weber M: New therapeutic aspects of flavones: The anti-cancer properties of *Scutellaria* and its main active constituents wogonin, baicalein and baicalin. *Cancer Treat Rev* 35: 57-68, 2009.
38. Li CM, He J, Gao YL, Xing YL, Hou J and Tian JW: Preventive effect of total flavones of *choerospondias axillaries* on ischemia/reperfusion-induced myocardial infarction-related MAPK signaling pathway. *Cardiovasc Toxicol* 14: 145-152, 2014.
39. Mu J, Liu T, Jiang L, Wu X, Cao Y, Li M, Dong Q, Liu Y and Xu H: The traditional chinese medicine baicalin potentially inhibits gastric cancer cells. *J Cancer* 7: 453-461, 2016.
40. Li Q, Ren FQ, Yang CL, Zhou LM, Liu YY, Xiao J, Zhu L and Wang ZG: Anti-proliferation effects of isorhamnetin on lung cancer cells in vitro and in vivo. *Asian Pac J Cancer Prev* 16: 3035-3042, 2015.



This work is licensed under a Creative Commons Attribution-NonCommercial-NoDerivatives 4.0 International (CC BY-NC-ND 4.0) License.